JOURNAL OF THE KOREAN ASTRONOMICAL SOCIETY
39: 107 ~ 114, 2006

MOLECULAR CLOUDS WITH PECULIAR VELOCITY IN THE OUTER LOCAL ARM

MIJU KANG[1,2], AND YOUNGUNG LEE[2]
[1]Department of Astronomy & Space Science, Chungnam National University, Daejeon 305-764, Korea
[2] Korea Astronomy and Space Science Institute, International Center for Astrophysics, Daejeon 305-348, Korea
E-mail:mjkang@kasi.re.kr
(Received November 27, 2006; Accepted December 22, 2006)

ABSTRACT

We conducted an analysis of a selected region from the FCRAO ^{12}CO Outer Galaxy Survey. The selected region is located between galactic longitude 117° and 124° with the velocity of -23 km s^{-1} $< V_{LSR} < -10$ km s^{-1} . Molecular clouds in this region show a peculiar velocity field, protruding from the Local Arm population. The selected region is divided into 7 clouds by spatial location. Though we were not able to identify the direct driving source for peculiar velocity of our target region, we find that there are several internal YSOs or star forming activities; there are many associated sources like an outflows, a high−mass protostellar candidate and H_2O maser sources. We attribute the driving energy source to older generation of episodic star formation. Masses of main clouds (cloud 1 − 4) estimated using a conversion factor from ^{12}CO luminosity are larger than $10^4 M_\odot$. Other components have a small mass as about $10^3 M_\odot$. Among main clouds, cloud 2 and 4 seem to be marginally gravitational bound systems as their ratio of M_{CO} to M_{VIR} is about 2~3, and the internal velocity dispersion is larger than the centroid velocity dispersion. Total mass estimated using a conversion factor from ^{12}CO luminosity is $7.9 \times 10^4 M_\odot$.

Key words : ISM : Outer Galaxy - ISM : structure - velocity objects : molecular clouds

I. INTRODUCTION

Molecular clouds are known to be located on the inner part of spiral arms. Though their major component is molecular hydrogen (H_2), the most widely used tracer of interstellar molecular gas is the carbon monoxide (CO), as H_2 does not have transition lines in low temperature of 10 K or so. Most of the molecular clouds do exist in the arm, and massive cloud seldom exist between the arms. Carey et al. (1995) reported in their second quadrant survey of molecular clouds that the interarm population is very small compared to arm components, and is dominated by smaller clouds. In addition, most of the mass of molecular gas in spiral arm is contained in the GMC's.

Early study of spiral arms (Cohen et al. 1980) showed that the Local arm is the lane of ^{12}CO clouds lying approximately in the velocity interval of 0 km s^{-1} to -20 km s^{-1}, and the Perseus arm in the parallel line at -40 km s^{-1} to -60 km s^{-1} along the galactic plane from $l = 105°$ to $l = 130°$. Recently, Heyer et al. (1998) presented the Local ($-20 < V_{LSR} < +4$ km s^{-1}) and Perseus arm ($-61 < V_{LSR} < -33$ km s^{-1}) velocity intervals based on the integrated ^{12}CO intensity.

In order to study physical properties of molecular clouds in the Outer Galaxy, we are planning a large−scale ^{13}CO ($J = 1 - 0$) survey using the Taeduk Radio Astronomy Observatory (TRAO) 14m telescope and a fifteen−beam receiver system, which is being installed. As a preliminary study, we have studied the existing database of FCRAO ^{12}CO Outer Galaxy Survey (OGS) (Heyer et al. 1998). While analyzing the spatial−velocity map of the FCRAO OGS database, we find that some clouds apparently have a peculiar velocity structure, protruding into the interarm region from the Local Arm(see Figure 1). The velocity range of molecular clouds located in $l = 117°$ to $l = 124°$ seems to be well separated from that of the Local Arm and show a special structure within the velocity range of -14 km s^{-1} to -23 km s^{-1}.

In this paper, we describe the structure and physical properties of these molecular clouds. We present data taking processes in section II. In section III, the estimate of distances to the molecular clouds and the derived physical properties are delineated. In section IV, we present the velocity structure of the target clouds and describe individual clouds in detail. In section V, we discuss the physical condition of molecular clouds, and summarize our conclusions in section VI.

II. DATA TAKING

We obtained all of slice (l, v) data (in unit of K, on the T_R^* scale) from the OGS (Heyer et al. 1998), and constructed a cube (l, b, v) for the whole surveyed region. This is comprised of 1,696,800 spectra sampled every $50''$ covering $l = 102.°49$ to $l = 141.°54$, and $b = -3.°03$ to $b = 5.°41$. Using the OGS, Brunt et

Corresponding Author: M. Kang

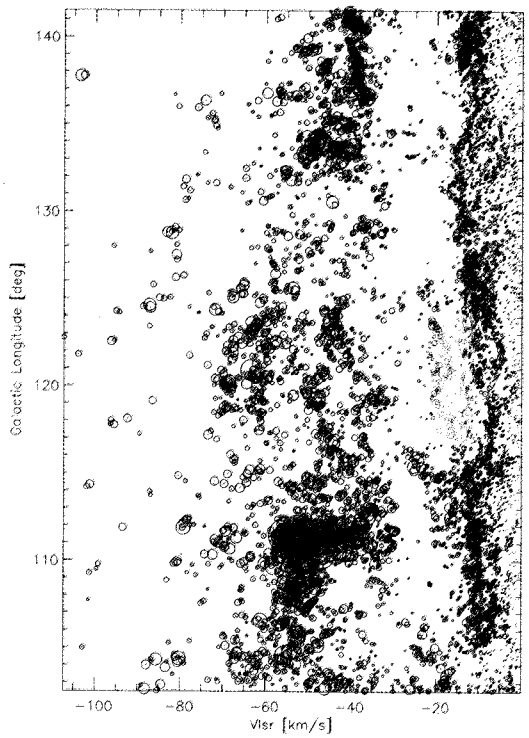

Fig. 1.— The spatial−velocity map of the identified molecular clouds in the Outer Galaxy Survey (Brunt et al. 2003). The size of the open circle represents mass of the molecular cloud. The colored circles represent the molecular clouds we are interested in.

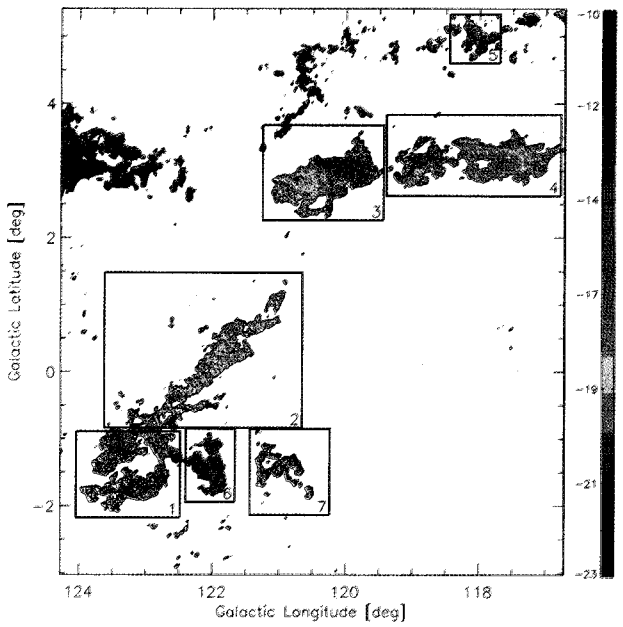

Fig. 2.— Emission weighted mean velocity map. The integration range is -10 km s^{-1} $< V_{LSR} <$ -23 km s^{-1} and 7 rectangles represent the individual clouds. Contour, representing boundary of the molecular clouds, is 5.0 K km s^{-1} (3σ). The scale bar is presented in units of km s^{-1}.

al. (2003) recently listed a catalog of molecular clouds identified with a revised clump−find method. The identified clouds are presented in longitude-velocity plot in Figure 1. Size of circle represents an arbitrarily scaled mass of a cloud. As we notified an ensemble of clouds, which is well distinguished from the Local Arm population as represented in color (Figure 1), we selected it as our target region for further study of analysis. The galactic longitude range of this region is 117° $\sim$ 124°, its galactic latitude range is $-3.°03$ to $5.°41$, and its velocity range is -10 km s^{-1} to -23 km s^{-1}; Our interested range of velocity is -14 km s^{-1} $\sim$ -23 km s^{-1} , but it is widened as its boundary is not clear around -10 km s^{-1} to -14 km s^{-1}.

In addition to CO data, we collected several associated catalogs, such as catalogs of OB associations, outflows and YSOs etc. from Centre de Donnes astronomiques de Strasbourg (CDS).

III. PHYSICAL PROPERTIES

For molecular clouds in the Outer Galaxy, their kinetic distances can be determined without any ambiguity. The kinetic distances of the clouds were estimated with a flat rotation curve of $R_0 = 8.0$ kpc and $\Theta_0 = 220$ km s^{-1}. Estimated kinematic distances to the clouds are ranging from 1 kpc to 1.4 kpc. Though distances of some of associated outflows had been reported as 850pc in other studies (Hodapp 1994; Wu et al. 2002; see Section IV), we will use kinematic distances for estimating their physical parameters.

The cloud mass has been estimated in two different ways: a mass estimate using virial theorem without including external pressure term, and a mass estimate obtained by using the CO luminosity (luminosity to mass conversion factor, or intensity to column density conversion factor). First, if a molecular cloud is gravitationally bound, then the partition of energy will be governed by the virial theorem. The virial mass estimate in this case is given by

$$M_{VIR} = \frac{3\beta\sigma_{tot}^2}{2G} D, \quad (1)$$

where D is the cloud diameter. The shape of the cloud is amorphous so that there is no definite way of defining a cloud size directly. We determine the mean cloud diameter ($D = \sqrt{(4A/\pi)}$), taking the area of the cloud (A) to be covered by all pixels with ^{12}CO integrated intensity greater than 3σ. The constant β is usually dependent on the density model of the cloud. Total

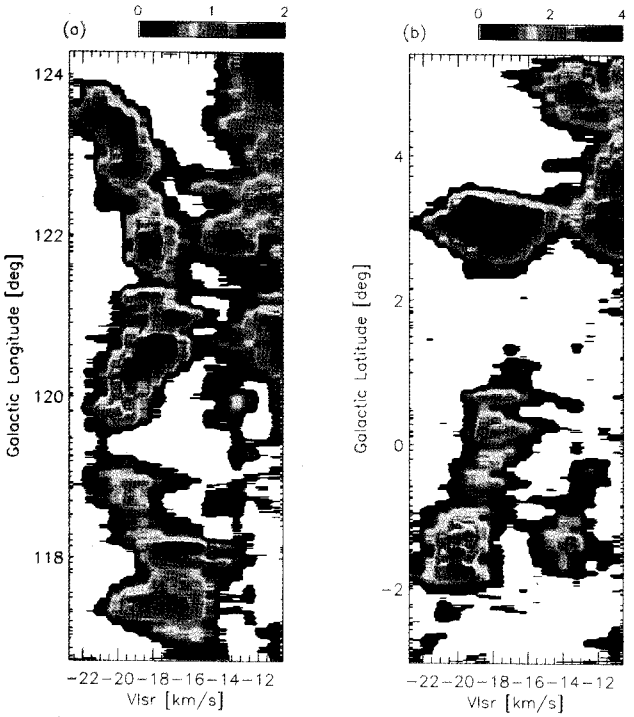

Fig. 3.— (a) The ^{12}CO longitude–velocity map integrated for the whole range of latitude observed. (b) The ^{12}CO latitude–velocity map integrated for the whole range of longitude. The scale bar is presented in units of K arcdeg.

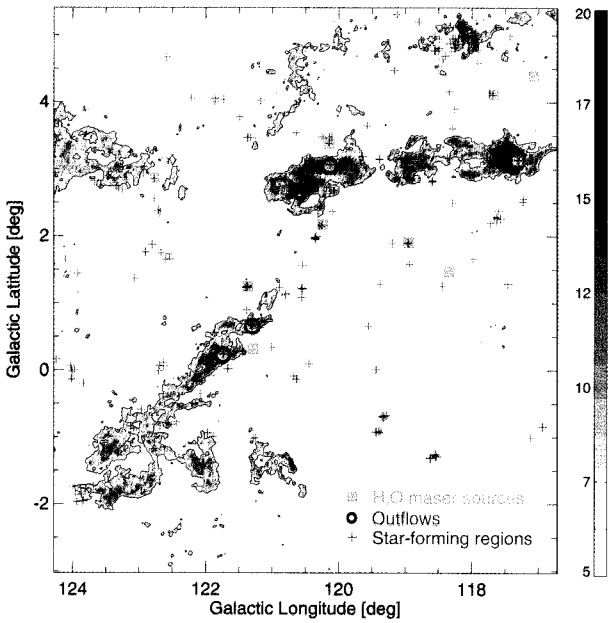

Fig. 4.— Velocity–integrated intensity map of the whole region. The integration range is -10 km s^{-1} $< V_{LSR} <$ -23 km s^{-1}. Contour is the 3σ value (5 K km s^{-1}). Filled squares are H_2O maser sources (Valdettaro et al. 2001), the cross symbols represent the star–forming regions in the solar neighborhood (Avedisova et al. 2002), and open red circles are the outflows reported by Hodapp (1994). The scale bar is presented in units of K km s^{-1}.

velocity dispersion of a cloud, σ_{tot}, can be decomposed to two terms (Lee et al. 1990); the first is an internal velocity dispersion (σ_i) which represents the spread of velocities observed along each line of sight, and the second is a centroid velocity dispersion (σ_c) which is usually associated with point-to-point bulk motion of the gas within the cloud. Thus, the total velocity dispersion of a cloud can be represented by $\sigma_{tot} = \sqrt{\sigma_i^2 + \sigma_c^2}$. If we assume a uniform density distribution and a spherical cloud ($\beta \sim 1.6$) and D is measured in pc and σ_{tot} in km s^{-1} (Lee et al. 1990):

$$M_{VIR} = 582\ D\ \sigma_{tot}^2 \quad [\mathrm{M}_\odot]. \qquad (2)$$

Another mass estimate can be obtained by using the relationship between the ^{12}CO integrated intensity and molecular hydrogen column density or equivalently the relationship between ^{12}CO luminosity and mass. We have used the conversion factor, $X = 1.9 \times 10^{20}$ cm^{-2} (K km s^{-1})$^{-1}$(Strong & Mattox 1996) in our calculations.

IV. RESULTS

(a) Large-scale morphology and velocity field

Figure 2 is the mean velocity map of the target region; its integrated velocity (V_{LSR}) range is from -10 km s^{-1} to -23 km s^{-1}, and the single contour of 5.0 K km s^{-1}(3σ) is presented, which helps to discriminate the individual cloud boundaries. Relatively clear boundaries of several clouds can be noticed except cloud 1 and 2 (see below). Brunt et al. (2003) used a modified clump-find algorithm to identify molecular clouds of the OGS. Their version of identified clouds is presented in Figure 1, and the number of clouds identified for our target region is more than 100. However, as one cloud tends to have more than one clump, their algorithm seems to be over dividing it into several smaller clouds or clumps. According to maps in Figures 2 and 3, fewer number of clouds is more likely. Thus, we arbitrarily divided the selected region into 7 individual clouds according to spatial distribution and velocity, without using any cloud identification code. We labeled them with numbers, such as cloud 1, cloud

2 etc.. In Figure 2 rectangle boxes are presented to mark the ranges of individual clouds. The physical properties and velocity fields of individual clouds are discussed in detail in section IV.

Upper part of mean velocity map (Figure 2), represented mainly in red and orange color, seems to be Local Arm population. The clouds in blue and green color are our target region. However, cloud 5 and cloud 6 are included for further analysis and comparison, though their velocity range differs a bit from that of target region; Our main clouds within the velocity range of -14 to -23 km s^{-1} are clouds $1-4$, and smaller one, cloud 7. Four main clouds $(1-4)$ is diagonally stretched on the middle of the Galactic plane.

In Figure 3 the velocity structure of the selected region is delineated in more detail. Figure 3(a) is a galactic longitude–velocity map integrated along galactic latitude direction, and Figure 3(b) is a galactic latitude–velocity map integrated along galactic longitude. Figure 3(a) shows that our target clouds are well separated from the Local Arm molecular clouds. An apparent arc-like structure might be noticed in this figure, for which one may expect some external driving source. This point will be discussed in later section. List of clouds are presented in Table 1. Column 1 is the cloud number and column 2 and 3 are their positions (l, b) of peak ^{12}CO emission, and the mean LSR velocity is presented in column 4. Column 5 is the peak temperature.

Table 2 represents estimated physical parameters. Column 2–4 are internal velocity dispersion, centroid velocity dispersion and total velocity dispersion. Column 5 is the kinematic distance from the Sun. Column 6 is the diameter of the cloud. Virial mass, ^{12}CO luminosity, and luminosity mass are listed in columns 7–9, respectively.

(b) Individual Clouds

i) Cloud 1

Cloud 1 and cloud 2 are weakly connected at the upper part of the cloud 1. As the morphology of two components is totally different (one for shell, and other for elongated structure), it might be more plausible to divide them into two, and to treat them separately.

The morphology of this cloud is substantially different from others; it has a clear shell-like structure with slight velocity gradient from -18 to -23 km s^{-1} (Figure 3(a)). There is an H II region Sh2-185 (Blitz 1982) closely located ($l = 123.^\circ97, b = -1.^\circ87$) to cloud 1. Its centroid velocity is -16.2 km s^{-1}, which is also close to the velocity range of cloud 1. Thus, there is some possibility that cloud 1 and the H II region are associated, as long as the physical location and velocity are concerned. This H II region was also noticed as LBN 620 and 622 (IC 59 and 63), which have been recognized as two distinct nebula separated about 20′ each other. In fact, these are small faint emission/reflection nebulae; IC 59 is larger and elongated N–S direction, but has much lower surface brightness than IC 63. IC 63 is distinct fan-shaped nebulosity extending to E and NE, and has a sharper edge at southern border (Gottlieb 1999; Cassiopeia recur 29 Jan 1999 Observing Report). On the other hand, there is an open cluster at ($l = 123.^\circ13, b = -01.^\circ29$), the same position of shell-like molecular cloud. Its spatial coverage is almost the same as that of cloud 1, and it comprised of stars with spectral types of B, A, F and G. Its central velocity is -9.55 km s^{-1}, and distance had been estimated as 750 pc (Kharchenko et al. 2005). Our kinematic distance estimate of 1.38 kpc to cloud is somewhat different from this open cluster, thus the possibility of direct association between two objects are less likely, though this issue is still open to be determined if our kinematic distance is substantially overestimated. In the meanwhile, the centroid velocity dispersion of the cloud is the second largest in our target region. In fact, the centroid velocity dispersion of the cloud 1 is 30% larger than the internal velocity dispersion. The total velocity dispersion is 1.81 km s^{-1}. This means that the cloud 1 is under more disturbed condition than others except cloud 3.

A few of IRAS point sources (see Figure 4) lie on the east–south boundary of the Cloud 1. IRAS point sources with flux density larger than 20 Jy at 100μm, and with smaller flux density at shorter wavelengths(60 and 25μm) are located within the cloud boundary, and especially a brighter IRAS point source (> 100 Jy at 100μm) lies on inside of the cloud. In the direction of cloud 1, ^{12}CO gases do not exist in other velocity range than our selected velocity range. Thus the bright IRAS point source could be a young stellar object within cloud 1. Star forming activity will be discussed in detail in Section V.

ii) Cloud 2

Cloud 2 is more elongated and filamentary than other clouds, and it is located diagonally on the Galactic Plane. Though there is a slight velocity gradient from east to west, any systematic movement is not likely. Its centroid velocity dispersion of $\sim$1 km s^{-1}

TABLE 1.
LIST OF CLOUDS

Name	l [deg]	b [deg]	V_{LSR} [km s^{-1}]	T_{pk} [K]
1	123.60	-1.41	-21.15	8.03
2	121.30	0.65	-18.72	13.37
3	120.67	2.63	-17.90	9.85
4	117.43	3.08	-16.27	13.12
5	117.95	4.95	-14.65	21.26
6	121.99	-1.39	-13.84	9.39
7	120.77	-1.27	-20.34	7.63

TABLE 2.
PHYSICAL PARAMETERS OF CLOUDS

Name	σ_i	σ_c	σ_{tot} [km s^{-1}]	distance [kpc]	size D [pc]	M_{VIR} [10^4 M$_\odot$]	L_{CO} [10^3 K km s^{-1} pc^2]	M_{CO} [10^4 M$_\odot$]
1	1.11	1.44	1.81	1.38	24.99	4.79	4.62	1.91
2	1.08	1.09	1.54	1.20	22.79	3.14	4.01	1.66
3	1.21	1.47	1.91	1.14	20.95	4.45	4.43	1.83
4	1.37	1.11	1.77	1.04	19.48	3.54	4.01	1.66
5	1.22	1.25	1.75	0.90	6.62	1.48	0.59	0.24
6	0.99	0.67	1.20	0.79	7.56	0.63	0.44	0.18
7	1.22	0.88	1.50	1.34	11.47	1.50	1.03	0.42

is relatively small, thus smaller external disturbance could be expected. However, two bright emission regions of the cloud (up to $T_R^* = 13.5$ K) are matched to molecular outflow sources (L1287 and L1293), detected by Hodapp (1994) and Wu et al. (2004) (see Figure 4). However, from the OGS database, we were not able to confirm that these have clear outflow features. This may be caused by less sensitive observation of OGS. In fact, the rms sensitivity per channel is 0.6 K for the whole database. In addition, there is one H_2O maser source at the cloud boundary, which is also a strong sign of star forming activity.

iii) Cloud 3

The longitude–velocity map in Figure 2 shows a clear velocity gradient from east (-16 km s^{-1}) to west (-22 km s^{-1}). Taking this cloud just as a single object, Cloud 3 might be modeled as a rotating object from west to east. For that reason the centroid velocity dispersion has the largest out of 7 clouds. In addition, two molecular outflows, IRAS 00259+6510 and IRAS 00213+6530, are residing within the cloud 3 boundary (Hodapp 1994; Wu et al. 2004; see Figure 4). As there is no other molecular gas in other velocity range, two outflows must be directly associated with cloud 3. These are also associated with the bright emission regions. A small arc-shaped structure at the bottom part of Cloud 3 might be associated with an outflow, IRAS 00259+6510 (see Figure 4). However, with just ^{12}CO (J=1-0) data of OGS we were not able to confirm it. Further sensitive observation for this region is needed to clarify this issue.

iv) Cloud 4

Cloud 4 is composed of two parts, which are weakly connected each other. In this study we are handling them as one cloud just for convenience. There is also a velocity gradient, direction of which is opposite to that of cloud 3. This cloud has one of the brightest CO emission clumps (T_R^* is up to 13 K) in this target region. At the western end of the cloud it has a high mass protostellar candidate, IRAS 23545+6508 (Williams et al. 2004) ($l = 117.°3, b = +03.°1$), which could be a strong sign of direct heating and internal disturbance. We estimate IR luminosity of this IRAS point source using the following equation for galactic source (Emerson 1988):

$$F_{\rm IR}(7-135\mu m) = 1.0\times10^{-14}(20.653 f_{12}+ 7.538 f_{25} + 4.578 f_{60} + 1.762 f_{100}) \quad [{\rm Wm}^{-2}], \quad (3)$$

where f_{12}, f_{25}, f_{60}, and f_{100} are the IRAS flux densities in Jy unit at 12, 25, 60, and 100 μm.

The luminosity is then

$$L_{\rm IR} = 3.127\times10^7 D^2 F_{\rm IR} \quad [{\rm L}_\odot], \quad (4)$$

where D is in pc and $F_{\rm IR}$ in Wm^{-2}. IRAS 2345+6508, whose IR fluxes are 22.07 Jy at 12μm, 93.16 Jy at 25μm, 755.70 Jy at 60μm, and 1060.00 Jy at 100μm. The IR luminosity (2275 $L_\odot$) of IRAS 23545+6508 is much larger than the average for T Tauri stars, and even larger than those of Herbig Ae/Be stars. A linewidth is about $\Delta V = 4.16$ km s^{-1} in cloud 4. The internal velocity dispersion (σ_i) and the centroid velocity dispersion (σ_c) is 1.37 km s^{-1} and 1.11 km s^{-1} , respectively. The internal velocity dispersion is larger than the centroid velocity dispersion since the IRAS 23545+6508 provides a direct heating source and internal disturbance. Other star–forming activities within cloud 4 has been reported: Valdettaro et al. (2001) found H_2O maser source in IRAS 23545+6508 which had the peak velocity, -27.30 km s^{-1}. Wu et al. (2004) reported a high velocity molecular outflow, where H_2O maser is located. Williams et al. (2004) also suggested that the distance of the cloud from the Sun was 1.4 kpc, which is very similar to our distance estimate.

v) Cloud 5

From Figure 2 and 3, it can be noticed that cloud 5 is clearly isolated from main large structure. The peak temperature at (l, b = 117.°95, 4.°95) is 21.26 K, which is much higher than those of our main target clouds. Many star–forming regions reported by

Avedisova (2002) around cloud 5. Cloud 5 has not only the strong emission but also wide velocity dispersion, though its size is relatively smaller. The virial mass of cloud 5 is larger than that estimated using the ^{12}CO luminosity. The ratio is over 5 which is the largest one among 7 clouds. It may imply that cloud 5 is more disturbed than the others, and not gravitationally bound. Physical properties of cloud 5 are listed in Table 2 for comparison with other clouds.

vi) Cloud 6

Cloud 6 are just physically located near to cloud 1. However, the velocity of cloud 6 is quite different from one of cloud 1, and not related. Physical properties of cloud 5 are listed in Table 2 for comparison with other clouds.

vii) Cloud 7

Cloud 7 spatially keeps aloof from cloud 1 and 2. Its morphology is very filamentary. The internal velocity dispersion is -1.22 km s^{-1} and the centroid velocity dispersion is 0.88 km s^{-1}. No strong IRAS point sources, or any other objects, has been reported to be associated with cloud 7.

V. DISCUSSION

Our initial goal of this study was to answer why the target region is protruding to interarm region, and why it has such distinct velocity range, quite different from that of the Local Arm population. Could there be any external driving source for this distinctness ? Or can it be identified ? To answer these questions, we searched for most of related catalogs and databases which can be obtained from CDS. For instance, any OB association could be a good candidate for external driving source. In fact, there is one OB association, Cas OB 7 centered on ($l = 122.°8, b = 1.°2$), which lies on the east−north side of cloud 1 and 2 with an extension of 100 pc (or angular size of $3° \times 3°$), taking its distance of 2 kpc (Cazzolato & Pineault 2003). They also detected a large half-shell in H I around Cas OB7, as well as in the infrared and partially in CO. This half-shell was found to be covering a range of 20 km s^{-1} but could reach 40 km s^{-1} when extrapolating to the whole shell. Using HI database, they wanted to check the association possibility between Cas OB 7 and our target region. The H I shell is ranging from -14.24 km s^{-1} to -38.98 km s^{-1}, being most distinguishable at -35.68 km s^{-1} as a filamentary shell around Cas OB7(Cazzolato and Pineault 2003). However, the distance of 2 kpc is too far from that of our target region, and its extent of 120 pc is not within the reachable range of distance to our region. Thus, we conclude that there may be no possibility of association between two objects. Except this OB association, we are not able to find other driving source. Internal sources, such as young stellar object candidates, and several outflows are only direct driving sources. However, these are small range sources, disturbing molecular gas only locally. Thus, only other possibility of driving source would be episodic remnant of older generation of star forming activity, or external turbulent flow. For example, Lee et al. (1994) studied the massive cold cloud G216-2.5 which had the huge velocity field without any direct driving source. They claimed that the source might be the episodic remnant of older generation of star formation.

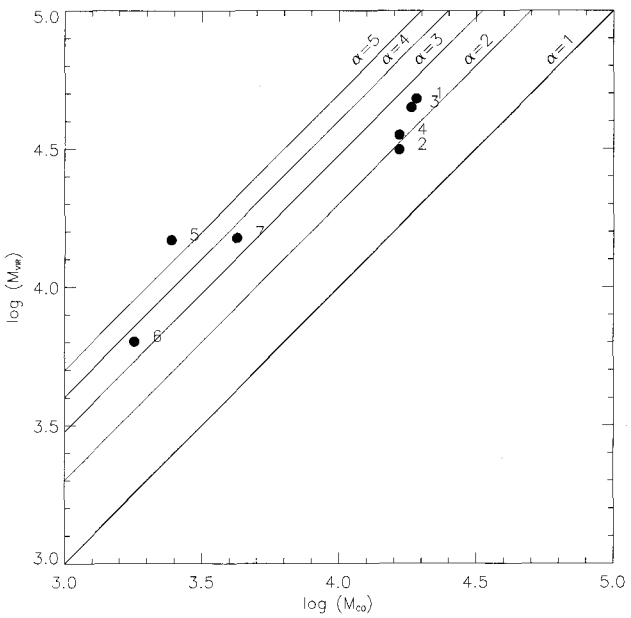

Fig. 5.— The $\log(M_{CO})-\log(M_{VIR})$ plot. Here the virial masses are plotted against those derived using a conversion factor, from ^{12}CO luminosity to gas mass. Lines represent the relation $\log(M_{CO}) = \alpha \log(M_{VIR})$

On the other hand, there is another possibility which should be studied further in larger scale; recently Kim and Ostriker (2006) reported that a magnetized spiral shock in a thin disk can undergo magneto-Jeans instability (MJI), resulting in regularly spaced interarm spur structures and massive gravitationally bound fragments. From Figure 1, there is some sign of spurs from the Local Arm population, especially at $l = 105°, 116°, 126°$, and $135°$, almost 10 degree apart one another. Our target region is located between $116°$ and $126°$ possible spurs. Though the spur study still remains to be seen for next a couple of years, the spacing of apparent spurs in Figure 1 is quite regular ($\sim$200 pc), assuming the kinematic distance of 1 kpc at the velocity of -20 km s^{-1}.

In the meanwhile, we estimate the masses using two different techniques. First, we assume that all clouds are a gravitationally bound system and ignoring external pressure term in the virial equation. Most of large molecular clouds ($M > 10^5 M_\odot$) are known to be in

virial equilibrium (gravitationally bound: Scoville et al. 1987). Generally, virial mass estimate tends to be larger than the other mass estimates. This issue had been discussed in detail by Lee (1994). Second, we find the luminosity mass (M_{CO}) based on the conversion factor($X = 1.9 \times 10^{20}\mathrm{cm}^{-2}(\mathrm{Kkms}^{-1})^{-1}$), which is being used most popularly. By comparing these two mass estimate, we can conjecture the condition of the gravitational boundness of target cloud. The plot of M_{VIR} versus M_{CO} for 7 clouds is presented in Figure 5. While cloud 2 and 4 are close to be gravitationally bound, the others may not be in gravitational boundness. Cloud 2 has a very similar centroid and internal velocity dispersion. In case of cloud 4, the internal velocity dispersion (1.37 km s^{-1}) is larger than the centroid velocity dispersion (1.11 km s^{-1}). It implies that the some disturbing source may exist within the cloud. In fact, cloud 4 has a high−mass protostellar candidate (IRAS 23545+6508) as mentioned above. However, cloud 1 and 3 have relatively large centroid velocity dispersion. This fact implies that the turbulent motions within clouds are large and molecular clouds are gravitational unbound. If size D is smaller than 10pc or a mass is small ($< 10^4 M_\odot$), the omitted external pressure term would become important as Heyer et al. (2001) and many other authors claimed that the isolated small molecular clouds required external pressures to maintain the equilibrium. Therefore, for small clouds like a cloud 5, 6, and 7, the proper mass should be definitely estimated by using coversion factor, which is the best mass estimate so far for any kinds of molecular clouds.

VI. SUMMARY

As a preliminary study of Outer Galaxy survey, we obtained a whole database from the FCRAO ^{12}CO Outer Galaxy Survey. We selected and analyzed the molecular clouds located between galactic longitude 117° and 124° with the velocity range of -23 km s^{-1} $< V_{LSR} < -10$ km s^{-1} . Clouds in this region show a peculiar velocity field protruding from the Local Arm population. The selected region is divided into 7 clouds by spatial location. The main clouds 1-4 is diagonally located in the middle of Galactic Plane. Though we were not able to find the direct driving source for our target region, we found that there are several internal YSOs or star forming activities; there are many associated sources like an outflows, high−mass protostellar candidate and H_2O maser sources. We attribute the driving energy source to older generation of episodic star formation. Other possibility, which still remain to be studied further, may be related to formation of spiral-arm spurs.

Masses of main clouds (cloud 1 − 4) estimated using a conversion factor from ^{12}CO luminosity are larger than $10^4 M_\odot$. Other components have a small mass as about $10^3 M_\odot$. Among main clouds, cloud 2 and 4 seem to be marginally gravitationally bound because the ratio between M_{CO} and M_{VIR} is about 2 and the internal velocity dispersion is larger than the centroid velocity dispersion. On the other hand, since the centroid velocity dispersions of Cloud 1 and 3 are larger than the internal velocity dispersions of them, two clouds may be not in gravitational boundness. Total mass estimated using a conversion factor from ^{12}CO luminosity is $7.9 \times 10^4 M_\odot$.

ACKNOWLEDGEMENTS

This work was supported by grant R01-2003-000-10513-0 from the Basic Research Program of the Korea Science and Engineering Foundation (KOSEF). We are grateful to Dr. W.-T. Kim (SNU) for discussion about spiral-arm spurs.

REFERENCES

Avedisova, V. S., 2002, A Catalog of Star−Forming Regions in the Galaxy, Astronomy Reports, 46, 193

Blitz, L., Fich, M., & Stark, A. A., 1982, Catalog of CO radial velocities toward galactic H II regions, ApJS, 49, 183

Brunt, C., Kerton, C. R., & Pomerleau, C., 2003, An Outer Galaxy Molecular Cloud Catalog, ApJS, 144, 47

Carey, S. J. 1995, Ph.D. thesis, Rensselaer Polytechnic Institute

Cazzolato, F., & Pineault, S., 2003, Large−Scale Structure and Dynamics of Cassiopeia OB7, AJ, 125, 2050

Cohen, R. S., Cong, H., Dame, T. M., & Thaddeus, P., 1980, Molecular clouds and galactic spiral structure, ApJ, 239, 53

Emerson, J.P., 1988 in Formation and Evolution of Low Mass Stars, edited by A.K. Dupree and M.T.V.T. Lago (Kluwer Academic, Dordrecht), Vol. 241, p. 193

Gottlieb, S., 1999, Cassiopeia recur 29 Jan 1999 Observing Report

Heyer, Mark H., Brunt, C., Snell, R. L., Howe, J. E., Schloerb, F. P., & Carpenter, J. M., 1998, The Five College Radio Astronomy Observatory CO Survey of the Outer Galaxy, ApJS, 115, 241

Heyer, M. H., Carpenter, J. M., & Snell, R. L., 2001, The Equilibrium State of Molecular Regions in the Outer Galaxy, ApJ, 551, 852

Hodapp, K-W., 1994. A K′ imaging survey of molecular outflow sources, ApJS, 94, 615

Kharchenko, N. V., Piskunov, A. E., Röser, S., Schilbach, E., & Scholz, R.-D., 2005, 109 new Galactic open clusters, A&A, 440, 403

Kim, W-T., & Ostriker, E. C., 2006, Formation of Spiral-Arm Spurs and Bound Clouds in Vertically Stratified Galactic Gas Disks, ApJ, 646, 213

Lee, Y., Snell, R. L., & Dickman, R. L., 1990, Analysis of ^{12}CO and ^{13}CO emission in a 3 square degree region of the Galactic plane between L = 23 deg and 25 deg, ApJ, 355, 536

Lee, Y., 1994, A Study of LYNDS 1251 Dark Cloud: I. Structure and Kinematics, JKAS, 27, 159

Scoville, N. Z., Yun, M. S., Sanders, D. B., Clemens, D. P., & Waller, W. H., 1987, Molecular clouds and cloud cores in the inner Galaxy, 63, 821

Strong, A. W., & Mattox, J. R., 1996, Gradient model analysis of EGRET diffuse Galactic $\gamma-$ray emission, A&A, 308, 21

Valdettaro, R., Palla, F., Brand, J., Cesaroni, R., Comoretto, G., Di Franco, S., Felli, M., Natale, E., Palagi, F., Panella, D., & Tofani, G., 2001, The Arcetri Catalog of H_2O maser sources: Update 2000, A&A, 368, 845

Williams, S. J., Fuller, G. A., & Sridharan, T. K., 2004, The circumstellar environments of high−mass protostellar objects. I. Submillimetre continuum emission, A&A, 417, 115

Wu, Y., Wei, Y., Zhao, M., Shi, Y., Yu, W., Qin, S., & Huang, M., 2004, A study of high velocity molecular outflows with an up−to−date sample, A&A, 426, 503